

# Sensorless Control for a Three-pole Active Magnetic Bearing System

Shyh-Leh Chen<sup>1</sup> and Kang-Yu Liu<sup>2</sup>

<sup>1</sup>Department of Mechanical Engineering and Advanced Institute of Manufacturing with High-tech Innovations  
National Chung Cheng University, Chiayi 621, Taiwan  
imeslc@ccu.edu.tw

<sup>2</sup>Motor Drive Solution BU  
Delta Electronics Inc., Taoyuan 330, Taiwan  
ken.yu.liu@deltaww.com

**Abstract** — This study proposes a novel sensorless control of a current-controlled three-pole active magnetic bearing (AMB) system. It is based on the smooth current controller incorporated with the estimated rotor displacements. The rotor position information is extracted from additional sensing coil currents. The sensing coil currents are generated from three phase voltages injected to the additional coils on each magnetic pole. The dynamic model of the 3-pole AMB with the additional high frequency input is derived for levitation control and for position estimation. The results are verified through simulation analysis.

**Index Terms** — Active magnetic bearing, sensorless control, smooth current control.

## I. INTRODUCTION

High speed and high accuracy are the major trends for machines in the 21<sup>st</sup> century. In this regard, active magnetic bearing (AMB) is an important element since it can provide noncontact suspension. This brings several important advantages, including a significant increase of the maximum rotation speed, friction-loss reduction, etc. However, the potential of its industrial applications has not been fully explored yet. One of the main reasons is its high cost. Therefore, cost reduction has always been an important research direction for the development of AMB system. Hardware accounts for the major part of the overall cost of an AMB. The elimination of some hardware requirements can substantially cut down the overall cost. The three-pole AMB was proposed for this particular purpose [1-4]. It has been shown that the three-pole AMB system requires less power amplifiers, possesses less copper and iron losses and provides more space for heat dissipation, coil winding and sensor installation.

To further reduce the overall cost, one may note that position sensors are in general more expensive than electrical sensors. It has been found that electrical signals

may be used to estimate the mechanical information [5], leading to the so-called self-sensing technique. Thus, sensor cost can be reduced.

In AMB system, the rotor displacement is the controlled variable, and thus, it must be measured or estimated. The rotor displacement is often measured using eddy-current sensors, which are the most widely used one for the magnetic bearing application [6]. It has the characteristics of small physical size with high resolution, excellent temperature stability, small phase shift and high dc stability. However, eddy current sensor has some drawbacks, including relatively high cost, as well as periodic calibration and maintenance requirements.

There have been a large number of self-sensing studies in the literature [7]. The nonlinear high-gain observer method was presented in [8], but the observer design is quite complex. The approach of pulse width modulation (PWM) switching power amplifiers was proposed in [9], [10], but this method requires good performance of PWM. Another approach is to inject a high frequency signal to the electromagnet wires [11], [12]. This signal is modulated by the varying air gap through the inductance of the coil. By demodulating the output signal with the frequency component of the injection signal, the air gap and thus the rotor displacements can be obtained. Some of the techniques have been well known in the field of motor control [13], but has been applied to AMB only recently.

This paper presents a new sensorless control technique for the three-pole AMB system. An additional coil on each magnetic pole is implemented for sensorless control. A three phase high frequency voltage is provided for the additional 3 coils. The current measurement of the additional coils and the original coils makes it possible to obtain the position of rotor.

This paper is organized as follows. After the introduction, the mathematical model of three-pole AMB system with additional coils is described and a smooth current controller is proposed in Section II. In

Section III, the rotor position estimation is proposed. Numerical simulations are carried out in Section IV to verify the design of additional coil three-pole AMB system. Finally, conclusions are drawn in Section V.

## II. SYSTEM MODELING AND SMOOTH CURRENT CONTROL

### A. Three-pole magnetic bearing model

The three-pole AMB considered here has been studied previously in [1-4, 14]. The three poles are arranged in a radially symmetric Y-shaped structure to produce a uniform force distribution in the 2-D configuration space. The upper two poles are wired together in a differential way so that only two independent coil currents and hence two power amplifiers are required. It has been shown in [1] that this configuration is the optimal design in the sense of minimum heat dissipation. In this section, in order to achieve sensorless control of the three-pole AMB, there will be an additional coil on each pole to provide three phase voltage source, as shown in Fig. 1. In other words, there are two sets of coils: control coils and sensing coils. The control coils for the upper two poles are wound in a differential way. In other words, the two poles share the same control current  $i_2$ , but with opposite winding directions (i.e.,  $i_3 = -i_2$ ). The magnetic circuit for the three-pole AMB is given by Fig. 2, assuming that the reluctances exist only on the air gaps. By simple circuit analysis, the magnetic flux passing through each pole, denoted by  $\phi_{is}$ , can be obtained as:

$$\phi_{1s} = \frac{(R_2 + R_3)N_1 I_1 - R_3 N_2 I_2 - R_2 N_3 I_3}{R_1 R_2 + R_2 R_3 + R_3 R_1}, \quad (1)$$

$$\phi_{2s} = \frac{-R_3 N_1 I_1 + (R_1 + R_3)N_2 I_2 - R_1 N_3 I_3}{R_1 R_2 + R_2 R_3 + R_3 R_1}, \quad (2)$$

$$\phi_{3s} = \frac{-R_2 N_1 I_1 - R_1 N_2 I_2 + (R_1 + R_2)N_3 I_3}{R_1 R_2 + R_2 R_3 + R_3 R_1}, \quad (3)$$

where  $N_1 I_1 = N_i + N_s i_{1s}$ ,  $N_2 I_2 = N_i + N_s i_{2s}$ ,  $N_3 I_3 = N_i + N_s i_{3s}$ ,  $N$  is the number of control coil turns on each pole,  $N_s$  is the number of sensing coil turns on each pole,  $i_1$  to  $i_3$  are the control coil currents,  $i_{1s}$  to  $i_{3s}$  are the sensing coil currents and  $R_1$  to  $R_3$  are the reluctances of the air gaps between the rotor and the three magnetic poles. The reluctance can be expressed by:

$$R_j = \frac{l_j}{\mu A}, \quad (4)$$

where  $l_1$  to  $l_3$  represent the air gaps,  $\mu$  is the magnetic permeability of the air and  $A$  is the face area of each pole.

The magnetic force of the three-pole AMB can be easily obtained. Assume that the magnetic characteristic is linear (i.e., linear B-H relationship) and fringing effects and flux leakage are neglected. Then, by

Ampere's law and principle of virtual work, the magnetic force is related to the magnetic flux by:

$$F_i = \frac{\phi_{is}^2}{2\mu A}, \quad i = 1 \sim 3. \quad (5)$$

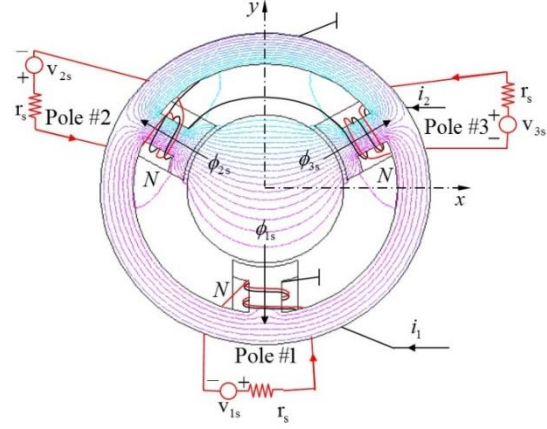


Fig. 1. The current-controlled three-pole AMB system with sensing coils.

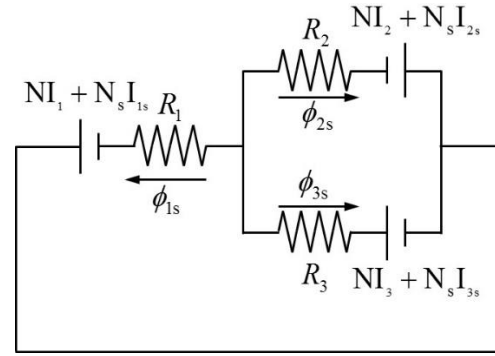


Fig. 2. Magnetic circuit for the additional coil three-pole AMB.

Using Newton's second law of motion, the magnetic force generated by the three poles in the X and Y directions are:

$$\ddot{x}_r = \frac{1}{m}(F_3 - F_2)\cos(30^\circ) = c_0 \Phi_{1s} \Phi_{2s}, \quad (6)$$

$$\ddot{y}_r = \frac{1}{m}[(F_3 + F_2)\sin(30^\circ) - F_1] - g = \frac{c_0}{2}(\Phi_{2s}^2 - \Phi_{1s}^2) - g, \quad (7)$$

where  $c_0 = \frac{4\mu A}{3m}$ ,  $m$  is rotor mass,  $\Phi_{1s}$  and  $\Phi_{2s}$  are defined by:

$$\Phi_{1s} = \frac{3}{4\mu A}(\phi_{3s} + \phi_{2s}), \quad (8)$$

$$\Phi_{2s} = \frac{\sqrt{3}}{4\mu A}(\phi_{3s} - \phi_{2s}). \quad (9)$$

## B. Coordinate transformations

Note that the magnetic fluxes  $\phi_{is}$  contain the contribution from both control and coil currents. Due to the differential winding configuration, there are only two independent control currents since  $i_3 = -i_2$ . On the other hand, the sensing coil currents  $i_{is}$  will be generated by the three phase voltages as shown in Fig. 1. That is, they need to satisfy the Faraday's induction law as:

$$\begin{bmatrix} v_{1s} \\ v_{2s} \\ v_{3s} \end{bmatrix} = r_s \begin{bmatrix} i_{1s} \\ i_{2s} \\ i_{3s} \end{bmatrix} + N_s \begin{bmatrix} \dot{\phi}_{1s} \\ \dot{\phi}_{2s} \\ \dot{\phi}_{3s} \end{bmatrix}, \quad (10)$$

where  $v_{1s}$  to  $v_{3s}$  are three phase voltage,  $r_s$  is coil resistance. Equation (10) can be transformed into the Cartesian coordinate through the inverse Clarke transformation:

$$\begin{bmatrix} f_a \\ f_b \\ f_c \end{bmatrix} = \begin{bmatrix} 0 & -1 \\ -\frac{\sqrt{3}}{2} & \frac{1}{2} \\ \frac{\sqrt{3}}{2} & \frac{1}{2} \end{bmatrix} \begin{bmatrix} f_x \\ f_y \end{bmatrix}, \quad (11)$$

to yield,

$$\begin{bmatrix} v_x \\ v_y \end{bmatrix} = r_s \begin{bmatrix} i_x \\ i_y \end{bmatrix} + N_s \begin{bmatrix} \dot{\phi}_x \\ \dot{\phi}_y \end{bmatrix}. \quad (12)$$

In other words,  $v_x, v_y$  are the transformed three phase voltages;  $i_x, i_y$  are the transformed sensing currents;  $\phi_x, \phi_y$  are the transformed magnetic fluxes on the three poles. It can be shown that Equations (8) and (9) will become:

$$\Phi_{1s} = \frac{3}{4\mu A} (\phi_{3s} + \phi_{2s}) = \frac{3}{4\mu A} \phi_y, \quad (13)$$

$$\Phi_{2s} = \frac{\sqrt{3}}{4\mu A} (\phi_{3s} - \phi_{2s}) = \frac{3}{4\mu A} \phi_x. \quad (14)$$

Thus, Equation (12) can be re-written as:

$$\begin{bmatrix} v_x \\ v_y \end{bmatrix} = r_s \begin{bmatrix} i_x \\ i_y \end{bmatrix} + \frac{4\mu AN_s}{3} \begin{bmatrix} \dot{\Phi}_{2s} \\ \dot{\Phi}_{1s} \end{bmatrix}. \quad (15)$$

Also, in terms of rotor displacements and coil currents, Equations (13) and (14) become:

$$\begin{bmatrix} \Phi_{1s} \\ \Phi_{2s} \end{bmatrix} = -\frac{N}{L} \begin{bmatrix} 2l_0 - y_r & \sqrt{3}x_r \\ x_r & \sqrt{3}(2l_0 + y_r) \end{bmatrix} \begin{bmatrix} i_1 \\ i_2 \end{bmatrix} - \frac{N_s}{L} \begin{bmatrix} -\frac{3}{2}x_r & -3l_0 + \frac{3}{2}y_r \\ -3l_0 - \frac{3}{2}y_r & -\frac{3}{2}x_r \end{bmatrix} \begin{bmatrix} i_x \\ i_y \end{bmatrix}, \quad (16)$$

where  $x_r$  and  $y_r$  are the rotor displacements,  $l_0$  is the nominal air gap and  $L = 4l_0^2 - (x_r^2 + y_r^2)$  is always

positive in the operation rang because that the rotor displacement is always smaller than the nominal air gap, i.e.,  $(x_r^2 + y_r^2) \leq l_0^2$ . Finally, let us define the system states as  $x_{1s} = x_r$ ,  $x_{2s} = \dot{x}_r$ ,  $x_{3s} = y_r$ ,  $x_{4s} = \dot{y}_r$ ,  $x_{5s} = \Phi_{1s}$ ,  $x_{6s} = \Phi_{2s}$ . That is,

$$x_s = [x_{1s} \ x_{2s} \ x_{3s} \ x_{4s} \ x_{5s} \ x_{6s}]^T.$$

Then, the system dynamics can be obtained as:

$$\dot{x}_s = \begin{bmatrix} x_{2s} \\ c_0 x_{5s} x_{6s} \\ x_{4s} \\ \frac{c_0}{2} (x_{6s}^2 - x_{5s}^2) - g \\ \frac{3}{4\mu AN_s} (v_y - r_s i_y) \\ \frac{3}{4\mu AN_s} (v_x - r_s i_x) \end{bmatrix}, \quad (17)$$

where  $v_x = V \cos \omega t$ ,  $v_y = V \sin \omega t$ ,  $V$  is the amplitude of the three phase voltage. The sensing currents depend on the rotor displacements and control currents, and can be obtained from Equation (16) as:

$$\begin{bmatrix} i_x \\ i_y \end{bmatrix} = \frac{2}{3N_s} \begin{bmatrix} -x_{1s} & 2l_0 - x_{3s} \\ 2l_0 + x_{3s} & -x_{1s} \end{bmatrix} \begin{bmatrix} x_{5s} \\ x_{6s} \end{bmatrix} + \frac{2N}{3N_s} \begin{bmatrix} 0 & \sqrt{3} \\ 1 & 0 \end{bmatrix} \begin{bmatrix} i_1 \\ i_2 \end{bmatrix}. \quad (18)$$

## C. Smooth current control

It is well known that the AMB system is unstable and nonlinear. As a result, it is necessary to design a stabilizing feedback controller for stable suspension. Following the smooth current controller proposed in [3], we will design a controller for this system. For more details on smooth current control, please refer to [3]. Let us first consider the rotor dynamics part in the overall state Equation (17), i.e.,

$$\dot{x}_s = \begin{bmatrix} x_{2s} \\ c_0 \Phi_{1s} \Phi_{2s} \\ x_{4s} \\ \frac{c_0}{2} (\Phi_{2s}^2 - \Phi_{1s}^2) - g \end{bmatrix}. \quad (19)$$

Regarding  $\Phi_{1s}$  and  $\Phi_{2s}$  as virtual control inputs, we can design a control law as:

$$\Phi_{1s} = \psi_1(x), \quad \Phi_{2s} = \sqrt{\frac{2g}{c_0}} + \psi_2(x), \quad (20)$$

$$\psi_1(x) = k_{11}x_{1s} + k_{12}x_{2s} + k_{13}z_1, \quad (21)$$

$$\psi_2(x) = k_{24}x_{3s} + k_{25}x_{4s} + k_{26}z_2, \quad (22)$$

where  $z_1 = \int x_{1s} dt$ ,  $z_2 = \int x_{3s} dt$ , and  $k_{ij}$ 's are the PID feedback gains. Therefore, from Equation (16), the overall control law for the control currents is given by:

$$\begin{bmatrix} i_1 \\ i_2 \end{bmatrix} = -\frac{1}{\sqrt{3}N} \begin{bmatrix} \sqrt{3}(2l_0 + x_{3s}) & -\sqrt{3}x_{1s} \\ -x_{1s} & 2l_0 - x_{3s} \end{bmatrix} \begin{bmatrix} \psi_1(x) \\ \sqrt{\frac{2g}{c_0}} + \psi_2(x) \end{bmatrix} \\ + \frac{N_s}{N} \begin{bmatrix} 0 & \frac{3}{2} \\ \frac{\sqrt{3}}{2} & 0 \end{bmatrix} \begin{bmatrix} i_x \\ i_y \end{bmatrix}. \quad (23)$$

Note that unlike the standard smooth current control [3], here the control currents need to compensate the disturbance from the sensing currents.

Comments on the computational issues of the feedback control law (23) are made here. An important parameter in the control law is  $c_0$ . It is related to the magnetic force model. In order to get accurate value, it is better to use finite element method for the model of magnetic forces [15]. It can also be obtained by experimental calibration of magnetic force model, as presented in [2].

### III. THE ROTOR DISPLACEMENT ESTIMATION

The estimation of rotor displacements will be based on Equation (16), or equivalently, Equation (18). It is the relationship between the rotor displacements and the electrical and magnetic quantities: the control currents  $i_1, i_2$ , the sensing currents  $i_x, i_y$ , and the equivalent magnetic fluxes  $\Phi_{1s}, \Phi_{2s}$ . Equation (18) can be re-written as:

$$i_x = \frac{(-2x_r\Phi_{1s} + 4l_0\Phi_{2s} - 2y_r\Phi_{2s} + 2\sqrt{3}Ni_2)}{3N_s}, \quad (24)$$

$$i_y = \frac{(4l_0\Phi_{1s} + 2y_r\Phi_{1s} - 2x_r\Phi_{2s} + 2Ni_1)}{3N_s}, \quad (25)$$

which is equivalent to:

$$x_r\Phi_{1s} + y_r\Phi_{2s} = 2l_0\Phi_{2s} + \alpha, \quad (26)$$

$$x_r\Phi_{2s} - y_r\Phi_{1s} = 2l_0\Phi_{1s} + \beta, \quad (27)$$

where  $\alpha = \sqrt{3}Ni_2 - \frac{3}{2}N_s i_x$  and  $\beta = Ni_1 - \frac{3}{2}N_s i_y$ . From

Equations (26) and (27), one can obtain the rotor displacements as:

$$x_r = \frac{1}{\Phi_{1s}^2 + \Phi_{2s}^2} (4l_0\Phi_{1s}\Phi_{2s} + \alpha\Phi_{1s} + \beta\Phi_{2s}), \quad (28)$$

$$y_r = \frac{1}{\Phi_{1s}^2 + \Phi_{2s}^2} (2l_0(\Phi_{2s}^2 - \Phi_{1s}^2) - \beta\Phi_{1s} + \alpha\Phi_{2s}). \quad (29)$$

In (28) and (29), the control currents  $i_1, i_2$  and sensing currents  $i_x, i_y$  can be measured by the current sensors.

Also, the equivalent magnetic fluxes  $\Phi_{1s}, \Phi_{2s}$  can be obtained by integrating Equation (15), i.e.,

$$\begin{bmatrix} \Phi_{1s} \\ \Phi_{2s} \end{bmatrix} = \frac{3}{4\mu AN_s} \int \left( \begin{bmatrix} v_y \\ v_x \end{bmatrix} - r_s \begin{bmatrix} i_y \\ i_x \end{bmatrix} \right) dt. \quad (30)$$

Therefore, Equations (28) and (29) can be used for the estimation of rotor displacements, and can be used for the feedback control in the smooth current controller (23).

Comments on the computational issues of position estimation algorithm (28) and (29) are made here. Note that the equivalent magnetic fluxes  $\Phi_{1s}, \Phi_{2s}$  are important quantities for the position estimation, as can be easily seen from (18) and (29). The computation of  $\Phi_{1s}, \Phi_{2s}$  using (30) could lead to large error if the transformed three-phase voltages  $v_x, v_y$  and the sensing currents  $i_x, i_y$  are contaminated with large noise. Therefore, a key point to obtain good estimation is to use filters to handle  $v_x, v_y$  and  $i_x, i_y$  before computing (30). An alternative way to get  $\Phi_{1s}, \Phi_{2s}$  is to use finite element method [15] to compute magnetic fluxes  $\phi_{is}$  and then use (13) and (14). This approach will yield more accurate  $\Phi_{1s}, \Phi_{2s}$ , but it is time-consuming and not feasible for real-time sensorless control.

### IV. SIMULATION RESULTS

To verify the effectiveness of the proposed sensorless control, numerical simulation will be carried out in this section. The nominal values of the system parameters are shown in Table 1. Note that the frequency of the sensing voltage is 100 Hz with amplitude of 1V. The control gains  $k_{ij}$ 's in (21) and (22) are designed using the method of pole placement. The closed-loop poles are chosen at:

$$\lambda_{11} = -28, \lambda_{12} = -25.5, \lambda_{13} = -13;$$

$$\lambda_{21} = -25.5, \lambda_{22} = -23, \lambda_{23} = -23.5;$$

where  $\lambda_{1i}$  represents the poles for the closed-loop linearized dynamics in the X-direction, and  $\lambda_{2i}$  for the Y-direction. The initial conditions for the system state  $x_s(0)$  is taken to be:

$$x_s(0) = \begin{bmatrix} 0 & 0 & -5 \times 10^{-4} m & 0 & 0 & 1 \times 10^{-2} \end{bmatrix}.$$

Note that there is a backup bearing placed on half way between the stator and the rotor. In other words, the practical allowable operation range for the rotor is a circle with radius of  $5 \times 10^{-4} m$ , which is marked by dashed lines in the following figure. Hence, the initial condition represents the situation that rotor is initially at rest on the backup bearing. The simulation results are shown in Fig. 3 and Fig. 4. Figure 3 shows the performance of the smooth current controller with the proposed rotor estimation scheme. Figures 3 (a) and 3 (b) indicate that the rotor can be levitated to the bearing center within 0.3 seconds. In Fig. 3 (c), the control

currents exhibit periodic oscillation to compensate for the sensing currents. Figure 4 shows the response of rotor displacement estimation and the estimation error. It indicates that both X and Y displacements can be estimated with good accuracy. The simulation results clearly verify the effectiveness of the proposed method.

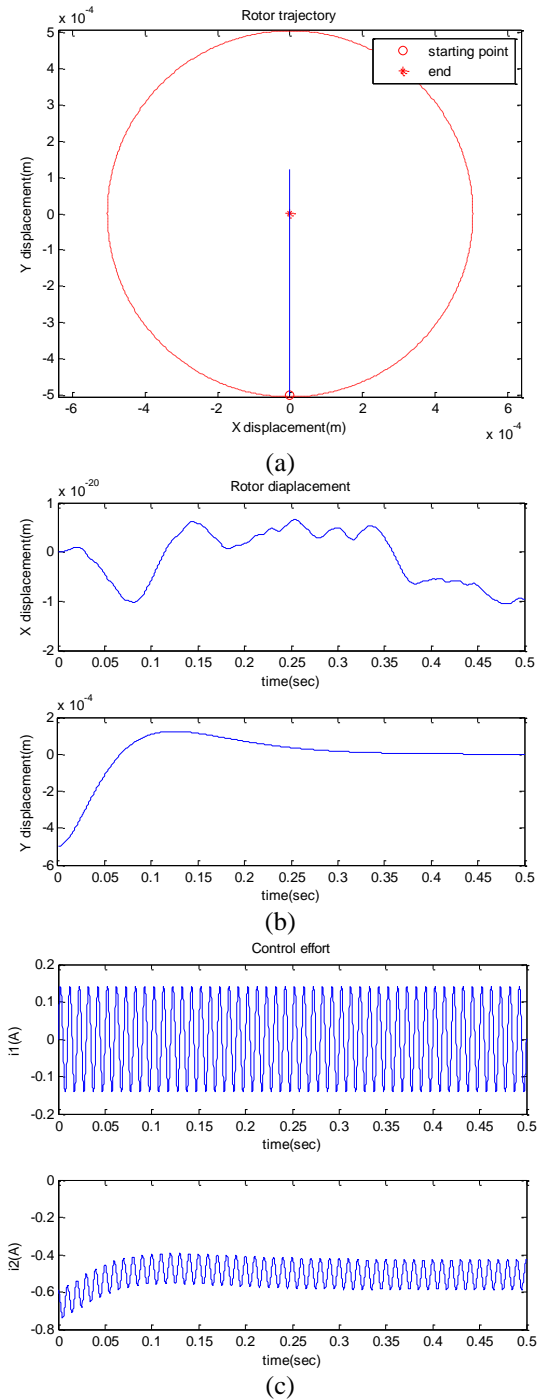


Fig. 3. Numerical simulations: (a) rotor trajectory with smooth current controller; (b) rotor displacements with smooth current controller; (c) control currents.

Table 1: Parameters of the AMB system

Rotor mass	0.6595kg
Nominal air gap	$0.95 \times 10^{-3} m$
Permeability	$4\pi \times 10^{-7} H/m$
Number of coil turns	300
Number of additional coil turns	20
Cross sectional area of the air gap	$4 \times 10^{-4} m^2$
Amplitude of sensing voltage	1V
Frequency of sensing voltage	100Hz
Resistance of additional coil turns	0.7056 $\Omega$

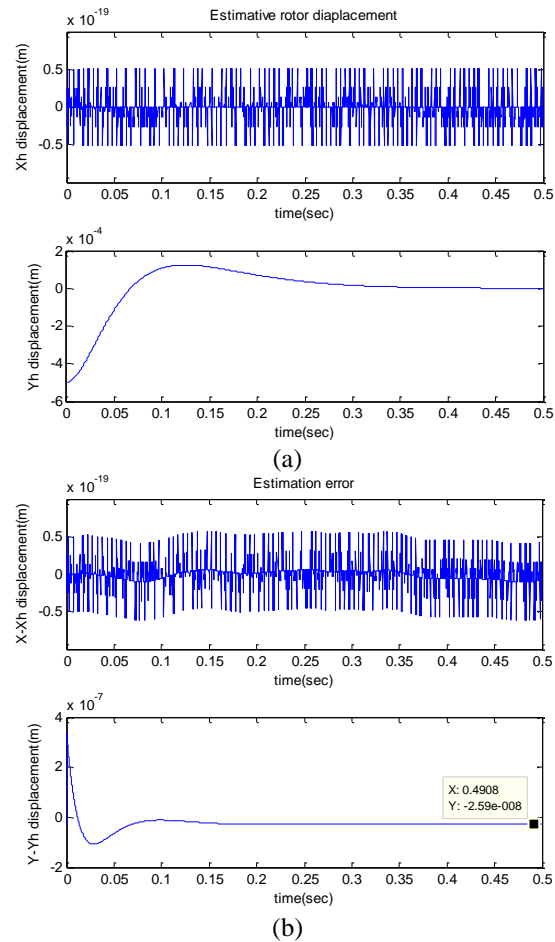


Fig. 4. Numerical simulations: (a) estimated rotor displacements; (b) estimation error.

## V. CONCLUSIONS AND FUTURE WORKS

A sensorless controller for a three-pole AMB system has been proposed in this study. It is based on the smooth current controller with additional three-phase sensing coil currents to estimate the rotor displacements. Numerical simulations verify the effectiveness of the proposed method. In the future, the stability of the closed-loop system will be analyzed and the experimental validation will be performed.

## ACKNOWLEDGMENT

This work was supported in part by the Ministry of Science and Technology, Taiwan, ROC, under Grants MOST 105-2218-E-194-003.

## REFERENCES

- [1] S. L. Chen and C. T. Hsu, "Optimal design of a three - pole active magnetic bearing," *IEEE Transactions on Magnetics*, vol. 38, no. 5, pp. 3458-3466, 2002.
- [2] S. L. Chen, S. H. Chen, and S. T. Yan, "Experimental validation of a current-controlled three-pole magnetic rotor-bearing system," *IEEE Transactions on Magnetics*, vol. 41, no. 1, pp. 99-112, 2005.
- [3] C. T. Hsu and S. L. Chen, "Exact linearization of a voltage-controlled 3-pole active magnetic bearing system," *IEEE Transactions on Control Systems Technology*, vol. 10, no. 4, pp. 618-625, 2002.
- [4] S. L. Chen, "Nonlinear smooth feedback control of a three-pole active magnetic bearing system," *IEEE Transactions on Control Systems Technology*, vol. 19, no. 3, pp. 615-621, 2011.
- [5] T. Mizuno, T. Ishii, and K. Araki, "Self-sensing magnetic suspension using hysteresis amplifiers," *Control Engineering Practice*, vol. 6, pp. 1133-1140, 1998.
- [6] J. Boehm, R. Gerber, and N. R. C. Kiley, "Sensors for magnetic bearings," *IEEE Transactions on Magnetics*, vol. 29, no. 6, pp. 2962-2964, 1993.
- [7] S. C. Mukhopadhyay, "Do we really need sensors? A sensorless magnetic bearing perspective," *1<sup>st</sup> International Conference on Sensing Technology*, Palmerston North, New Zealand, pp. 425-431, November 21-23, 2005.
- [8] S. L. Chen and Y. H. Hsiao, "Nonlinear high-gain observer for a three-pole active magnetic bearing system," in *Proc. ASCC*, pp. 155-159, 2011.
- [9] L. Lichuan, T. Shinshi, and A. Shimokohbe, "State feedback control for active magnetic bearings based on current change rate alone," *IEEE Transactions on Magnetics*, vol. 40, no. 6, pp. 3512-3517, 2004.
- [10] J. Wang and A. Binder, "Self-sensing magnetic bearings using multiple sampling of currents alone," in *Proc. IEEE EPE*, pp. 1-10, 2013.
- [11] J. S. Yim, J. H. Kim, S. K. Sul, H. J. Ahn, and D. C. Han, "Sensorless position control of active magnetic bearing based on high frequency signal injection method," in *Proc. IEEE APEC*, pp. 83-88, 2003.
- [12] P. Garcia, J. M. Guerrero, F. Briz, and D. Reigosa, "Sensorless control of three-pole active magnetic bearings using saliency-tracking-based methods," *IEEE Transactions on Industry Applications*, vol. 46, no. 4, pp. 1476-1484, 2010.
- [13] T. Yuvaraja and K. Ramya, "Vector control of PMSM take over by photovoltaic source," *ACES Express Journal*, vol. 1, no. 6, pp. 193-196, June 2016.
- [14] E. Schmidt and M. Hofer, "Application of the sliding surface method with 3D finite element analyses of a hybrid magnetic bearing," *25th Annual Review of Progress in Applied Computational Electromagnetics (ACES)*, Monterey, California, pp. 440-445, March 2009.
- [15] G. Liu, Y. Zhou, R. Zhou, W. Ming, and L. Huo, "Analysis and optimization of a 2-D magnet array with hexagon magnet," *Applied Computational Electromagnetics Society Journal*, vol. 28, no. 10, pp. 976-983, October 2013.



**Shyh-Leh Chen** was born on October 25, 1964, in Keelung, Taiwan. He received B.S and M.S. degrees from National Tsing-Hua University, Hsin-Chu, Taiwan, in 1987 and 1989, respectively, both in Power Mechanical Engineering. He received a Ph.D. degree in Mechanical Engineering from Michigan State University, East Lansing, Michigan, USA, in 1996.

Since 1996, he has been with National Chung Cheng University, Chiayi, Taiwan, where he is currently a Professor in the Department of Mechanical Engineering and a Deputy Director of Advanced Institute of Manufacturing with High-tech Innovations (AIM-HI). He also served as the Director of Advanced Machine Tools Research Center from 2010 to 2013. His research interests include nonlinear dynamics and control, wavelet analysis, with application to motion control of multi-axis systems, active magnetic bearings, and ship stabilization.



**Kang-Yu Liu** received the M.S. degree in Mechanical Engineering from National Chung Cheng University, Chiayi, Taiwan, R.O.C., in 2014. Currently, he is an R&D Engineer at Delta Electronics. His research interests include modeling, design, control and applications of

active magnetic bearing systems.